which are monomeric in their compounds. Apparently the electron-withdrawing character of the fluoro ligand and the relatively greater electropositive character of Te(IV) and I(V) compared to Xe(VI) favor the formation of bridges between anions.

Acknowledgment. The author is grateful for the hospitality and helpful discussions with Dr. A. Ruoff, Department of Chemistry, University of Ulm, Ulm, Germany, where part of this work was carried out. The author also thanks the Deutsche Akademische Austausch Dienst for financial assistance and the Canadian Department of External Affairs for the award of a travel grant.

Registry No. $KSeO_2F$, 15190-23-5; $CsSeO_2F$, 16004-28-7; Me_4NSeO_2F, 67891-59-2; Et_4NSeO_2F, 67891-60-5; $NaTeO_2F$, 67904-80-7; $KTeO_2F$, 67904-81-8; Me_4NTeO_2F, 67904-83-0.

References and Notes

(1) J. B. Milne and D. Moffett, *Inorg. Chem.*, **12**, 2240 (1973).
(2) R. J. Gillespie, P. Spekkens, J. B. Milne, and D. Moffett, *J. Fluorine Chem.*, **7**, 43 (1976).
(3) K. O. Christe, E. C. Curtis, C.J. Schack, and D. Pilipovich, *Inorg. Chem.*, **11**, 1679 (1972).
(4) R. Paetzold and K. Aurich, *Z. Anorg. Allg. Chem.*, **335**, 281 (1965).
(5) R. Paetzold and K. Aurich, *Z. Anorg. Allg. Chem.*, **348**, 94 (1966).
(6) L. B. Asprey and N. A. Matwiyoff, *J. Inorg. Nucl. Chem., Suppl.*, 123 (1976).
(7) C. J. Adams and A. J. Downs, *J. Chem. Soc. A*, 1534 (1971).
(8) R. Sabbah and C. Perinet, *J. Chim. Phys. Phys.-Chim. Biol.*, **63**, 332 (1966); ASTM File Card No. 21-644.
(9) P. A. Bazhulin, T. P. Mysasnikova, and A. V. Rakov, *Sov. Phys.—Solid State (Engl. Transl.)*, **5**, 1299 (1964).
(10) G. Lucovsy, A. Mooradian, W. Taylor, G. B. Wright, and R. C. Keezer, *Solid State Commun.*, **5**, 113 (1967).
(11) R. W. G. Wyckoff, "Crystal Structures", Vol. II, Interscience, New York, 1960, Section VII.
(12) J. B. Milne and D. Moffett, *Inorg. Chem.*, **13**, 2750 (1974).
(13) V. P. Cheremisinov and V. P. Zlomanov, *Opt. Spectrosc. (USSR)*, **12**, 208 (1962).
(14) H. A. Carter and F. Aubke, *Inorg. Chem.*, **10**, 2296 (1971).
(15) B. R. Nielsen, R. G. Hazell, and S. E. Rasmussen, *Acta Chem. Scand.*, **25**, 3037 (1971).
(16) R. J. Gillespie, B. Landa, and G. J. Schrobilgen, *Inorg. Chem.*, **15**, 1256 (1976).

Contribution from the Department of Chemistry, McMaster University, Hamilton, Ontario L8S 4M1, Canada

Preparation, Spectroscopic Properties, and Structure of the Pentabismuth(3+) Cation, Bi_5^{3+}

ROBERT C. BURNS, RONALD J. GILLESPIE,* and WOON-CHUNG LUK

Received May 25, 1978

The oxidation of bismuth with PF_5, AsF_5, SbF_5, $SbCl_5$, HSO_3F, and HSO_3Cl has been studied in SO_2 as the solvent. It was found that the pentafluorides oxidize bismuth first to Bi_8^{2+} and then to Bi_5^{3+}, but no evidence for polyatomic cations of bismuth was obtained in the reactions with the other oxidants. The new compound $Bi_5(AsF_6)_3 \cdot 2SO_2$ was isolated and characterized. The Raman and infrared spectra of the compounds $Bi_5(AsF_6)_3 \cdot 2SO_2$ and $Bi_5(AlCl_4)_3$ have been obtained and interpreted to show that the Bi_5^{3+} cation has a trigonal-bipyramidal structure. A complete vibrational analysis was carried out which indicates that the axial–equatorial bonds are somewhat stronger than the equatorial–equatorial bonds, with force constants of ~0.73 and ~0.55 mdyn/Å, respectively.

Introduction

The chemistry of bismuth in oxidation states of 1+ and lower has been rather extensively studied in investigations of the systems Bi–$BiCl_3$ and Bi–$BiCl_3$–MCl_x, where MCl_x is a metal chloride such as $AlCl_3$. The results of emf[1] and spectroscopic[2,3] studies of solutions of bismuth in $BiCl_3$ have been interpreted as indicating the formation of the species Bi^+ and $Bi_3^+ \cdot nBi^{3+}$. A compound isolated from these Bi–$BiCl_3$ melts was originally thought to be the monochloride[4] "BiCl" but was later shown to have the composition $Bi_{24}Cl_{28}$ and to have a structure consisting of Bi_9^{5+} cations accompanied by $BiCl_5^{2-}$ and $Bi_2Cl_8^{2-}$ anions.[5] The Bi_9^{5+} cation has also been found in the compound $Bi_{10}Hf_3Cl_{18}$, which has been isolated from the Bi–$BiCl_3$–$HfCl_4$ melt system. This was shown to be $Bi^+Bi_9^{5+}(HfCl_6^{2-})_3$ by an X-ray crystallographic study.[6] Spectroscopic studies on solutions of Bi and $BiCl_3$ in molten NaCl–$AlCl_3$ and KCl–$ZnCl_2$ eutectics have led to the identification of the cations Bi_5^{3+} and Bi_8^{2+} in addition to Bi^+.[7,8] The solid salts $Bi_5(AlCl_4)_3$ and $Bi_8(AlCl_4)_2$ were subsequently isolated by Corbett and shown to have reflectance spectra similar to the absorption spectra of Bi_5^{3+} and Bi_8^{2+} in the molten salt solutions.[9] The structures of Bi_5^{3+} and Bi_8^{2+} were not determined in this earlier work although simplified LCAO–MO calculations suggested that the former has a trigonal-bipyramidal geometry and that the latter has a square-antiprismatic structure.[9]

More recently the reactions of SbF_5 and AsF_5 with sulfur, selenium, or tellurium in SO_2 as a solvent have been used to prepare a large variety of polyatomic cations such as S_8^{2+}, Se_4^{2+}, Te_6^{4+}, $Te_2Se_8^{2+}$, $Te_3S_3^{2+}$, and $Te_2Se_4^{2+}$.[10-14] Many of these cations have also been prepared by the reactions of their respective elements with the very strong acids HSO_3F and $H_2S_2O_7$.[15,16] In every case it appears that stable solutions or stable crystalline salts of these polyatomic cations can only be obtained when the cation is accompanied by a large, very weakly basic anion such as $AlCl_4^-$, SbF_6^-, or SO_3F^-. The object of the present work was to study the oxidation of bismuth with a variety of oxidants in solution in SO_2 to investigate the formation of bismuth polyatomic cations in this medium, with the particular objective of obtaining more information on the structures of Bi_5^{3+}, Bi_8^{2+}, and any other bismuth cations that might be formed.

Experimental Section

Materials. Bismuth metal (200 mesh), as obtained from Alfa Inorganics, was indicated to be 99.999% pure and was used without further purification.

Commercial bismuth trichloride was dehydrated under vacuum at 140 °C and sublimed five times under a dynamic vacuum. The product so obtained was pure white, with no indication of carbonaceous impurity.[6]

0020-1669/78/1317-3596$01.00/0

Aluminum trichloride was sublimed three times in a static vacuum, after an initial sublimation from aluminum shot to remove the iron impurity.

Phosphorus pentafluoride and arsenic pentafluoride (Ozark Mahoning Co.) were used directly from their cylinders.

Antimony pentafluoride (Ozark Mahoning Co.) was doubly distilled in a Pyrex glass still in an atmosphere of dry nitrogen. Only the fraction boiling between 142 and 143 °C was collected.

Antimony pentachloride (99.2%, J. T. Baker Chemical Co.) and chlorosulfuric acid (99.5%, BDH) were used without further purification.

Technical grade fluorosulfuric acid (Baker and Adamson) was purified by double distillation as described by Barr.[17]

Anhydrous sulfur dioxide (Matheson of Canada) was distilled from a glass vessel containing P_4O_{10}, over which it had been stored for at least 24 h before use.

Sulfuric acid (100%) was kindly provided by Dr. T. Birchall, of this department. It had been prepared by adding 30% oleum to commercial sulfuric acid (95.5%) until the freezing point reached a maximum. Deuterosulfuric acid (98%, 99 atom % D) was obtained from Merck, Sharp and Dohme of Canada Ltd.

Reactions of Bismuth Metal with Oxidants. The oxidation of bismuth metal was studied using the oxidants PF_5, AsF_5, SbF_5, $SbCl_5$, HSO_3F, and HSO_3Cl. Reactions were carried out in double ampules with SO_2 as solvent, as described previously.[18] Approximately 0.2 g of bismuth metal and an approximately equimolar amount of oxidant were used in each reaction. The oxidant was either condensed into the reaction vessel or added directly by means of a syringe. After isolation, all solids were handled in a Vacuum Atmospheres Corp. drybox, Model HE-43, equipped with a drying train, Model HE-373-B, and were characterized by chemical analysis or spectroscopic procedures.

Synthesis of $Bi_5(AsF_6)_3 \cdot 2SO_2$ and $Bi_5(AlCl_4)_3$. (a) $Bi_5(AsF_6)_3 \cdot 2SO_2$. In a typical experiment arsenic pentafluoride (0.932 mmol) was condensed onto bismuth metal (1.036 mmol) in about 80 cm^3 of frozen SO_2 at −196 °C, and the reaction mixture was allowed to warm to room temperature. After about 2 h, the formation of a yellow precipitate was observed, but complete dissolution of the bismuth metal required up to 3 days. The volatiles AsF_3 and SO_2 were then removed under vacuum leaving a bright yellow solid. Anal. Calcd for $Bi_5(AsF_6)_3 \cdot 2SO_2$: Bi, 60.06; As, 12.92; F, 19.66; SO_2, 7.36. Found: Bi, 60.03, 59.90; As, 12.57, 12.65; F, 19.49, 19.68; SO_2 (by difference), 7.91, 7.77. The presence of SO_2 in the sample was confirmed by both Raman and infrared spectroscopic studies, as described below. The reaction between bismuth metal and AsF_5 may therefore be written

$$10Bi + 9AsF_5 \xrightarrow{SO_2} 2Bi_5(AsF_6)_3 \cdot 2SO_2 + 3AsF_3$$

Later, it was found that $Bi_5(AsF_6)_3 \cdot 2SO_2$ could best be prepared by adding slightly more than the required amount of AsF_5 to the metal. In this way reaction proceeded much faster and although there was some further oxidation of Bi_5^{3+} to Bi(III), the polyatomic species could easily be washed free of this impurity with SO_2, in which the latter is quite soluble.

(b) $Bi_5(AlCl_4)_3$. This compound was prepared according to the method of Corbett,[9,19] by fusing Bi, $BiCl_3$, and $AlCl_3$ in the stoichiometry given in eq 1 An X-ray powder diffraction pattern of the

$$4Bi + BiCl_3 + 3AlCl_3 \rightarrow Bi_5(AlCl_4)_3 \quad (1)$$

product was identical with that reported previously,[9,20] as was the diffuse reflectance spectrum. The solution of $Bi_5(AlCl_4)_3$ in $NaAlCl_4$ (~6 mol %) that was used in the spectroscopic work was also prepared in a similar manner, after a prior fusion at about 150 °C to avoid sublimation of $AlCl_3$ or $BiCl_3$.[9]

Spectra. Raman spectra were obtained using a Spex Industries Model 1400 spectrometer employing a double-monochromater and a phototube detector with an electrometer amplifier and recorder. For the solid samples, the exciting radiation was the red 6328-Å line of a Spectra-Physics 125 He–Ne laser while for the solution work the green 5145-Å line of a Spectra-Physics Model 140 Ar^+ laser was employed. The solid samples were sealed in $^1/_4$-in. o.d. Pyrex tubes and, to avoid decomposition, were spun in a rotating cell while the spectra were recorded. For the solution work, the sample was contained in a $^3/_4$-in. o.d. quartz tube mounted in a clear glass Dewar. A stream of air, which was heated by a nichrome resistance wire, was passed around the tube, and the temperature could be varied between room temperature and about 200 °C by altering the rate of flow. Temperatures were monitored using a copper–constantan thermocouple placed near the sample and, once a rate of air flow had been established, were found to be constant to better than 2 °C.

Infrared spectra over the range of 4000–200 cm^{-1} were recorded on a Perkin-Elmer grating infrared spectrometer, Type 283, with the samples mounted as Nujol mulls between CsI windows. The Nujol had been dried and then stored over sodium. Infrared spectra below 200 cm^{-1} were recorded using either an R.I.I.C. Fourier spectrometer FS-720 complete with a D.G.C. Nova 2 minicomputer or a Nicolet 7199 FT-IR system. The samples were mounted as Nujol mulls or powders in thin polyethylene packets which were heat sealed after the compounds had been introduced. Raman and FT-IR spectra as reported are accurate to ±1 cm^{-1}, while the grating spectrometer is accurate to ±1.5 cm^{-1} over the region of interest.

Absorption spectra were obtained using 1-cm rectangular silica cells and were recorded on a Cary 14 instrument against a reference cell containing solvent. All solutions were prepared and handled in the drybox. Electronic diffuse reflectance spectra were recorded using a Beckman DK-2A ratio recording spectrophotometer, together with a standard reflectance attachment. The samples were contained in airtight cells similar to those described by Reid, Scaife, and Wailes.[21]

X-ray Powder Data. Powder diffraction data were obtained from samples sealed in thin-walled Pyrex capillaries using an 11.46-cm diameter Philips Debye–Scherrer camera with nickel filtered Cu Kα radiation.

Analyses. Analyses were carried out by Alfred Bernhardt Mikroanalytisches Laboratorium, 5251 Elbach über Engelskirchen, West Germany.

Results and Discussion

Reactions of Bismuth Metal with Various Oxidizing Agents. The oxidation of bismuth metal was studied using PF_5, AsF_5, SbF_5, $SbCl_5$, HSO_3F, and HSO_3Cl as oxidants in SO_2 as a medium. A variety of products containing bismuth in different oxidation states were obtained depending on the strength of the oxidant and the reaction time.

The reaction of bismuth metal with PF_5 gave an initial, insoluble dark olive green solid after about 1 week, together with a little unreacted metal. A reflectance spectrum of this material identified the cation as Bi_8^{2+},[9] while an infrared spectrum indicated the presence of the hexafluorophosphate anion. Further oxidation of this material gave a yellow-brown solid, which was found to contain the Bi_5^{3+} cation from its reflectance spectrum. However, after several weeks bismuth metal was still present, even when a large excess of PF_5 was used. In view of the difficulty of isolating pure products, no further work was attempted on this system.

The reactions of AsF_5 and SbF_5 led to the preparation of the hexafluoroarsenate and hexafluoroantimonate salts of Bi_5^{3+}, the former being isolated as $Bi_5(AsF_6)_3 \cdot 2SO_2$. These reactions also passed through an olive green intermediate, presumably Bi_8^{2+}, but this reacted so quickly that isolation was impossible. The reaction with SbF_5 gave a similar product to that of the reaction with AsF_5, but the salt could not be separated from the reduction product, SbF_3, which is also insoluble in SO_2. Separation of the products by vacuum distillation of the SbF_3 at 120 °C was attempted, but this led to decomposition of the cation to bismuth metal, probably by a disproportionation reaction so that some trivalent bismuth was formed as well. Further oxidation of the hexafluoroarsenate and hexafluoroantimonate salts with AsF_5 and SbF_5, respectively, gave products containing only trivalent bismuth.

With a large excess of the oxidants $SbCl_5$, HSO_3F, and HSO_3Cl, reaction always gave white crystalline products; if a large excess of oxidant was not used, unreacted metal was also present. Similar reactions also occurred when HSO_3F and HSO_3Cl were used in the absence of SO_2. No evidence could be obtained for the formation of polyatomic cations of bismuth in any of these reactions and the white solids presumably contained trivalent bismuth, although this was only verified in the case of the reaction with $SbCl_5$.

Table I. The Electronic Spectrum of the Bi_5^{3+} Cation[a]

$Bi_5(AsF_6)_3 \cdot 2SO_2$			$Bi_5(AlCl_4)_3$		
absorption spectrum (100% H_2SO_4)			absorption spectrum[b] ($NaAlCl_4$, 130 °C)		
λ, nm	$10^3\epsilon$, dm^3 cm^{-1} mol^{-1}	reflectance spectrum, nm	λ, nm	$10^3\epsilon$,[d] dm^3 cm^{-1} mol^{-1}	reflectance and mull spectra,[c] nm
821	0.18	810	875	0.5	805
720	0.11	~710 sh[e]	770	0.3	~730 sh
~525	0.29		~540	1.0	540
		460 sh			
425 br	1.05	426	~455	2.9	455
		385 sh			
362	2.39	358	390	6.5	390
		325			345
		295			305
~275 sh[f]					

[a] All spectra recorded at room temperature, unless otherwise indicated. [b] References 7 and 8. [c] Reference 9 and this work. [d] Estimated from spectra reported in ref 7 and 8. [e] sh = shoulder, br = broad. [f] Assigned to SO_2, but see text.

In this study the only cations that were isolated were Bi_8^{2+}, Bi_5^{3+}, and Bi^{3+} and no evidence could be found for the existence of Bi^+, Bi_9^{5+}, or any other previously unidentified polyatomic cations of bismuth. Interestingly, the cations Bi_8^{2+} and Bi_5^{3+} were only observed when the counteranions were derived from the group 5 pentafluorides. It is somewhat surprising that these cations, or perhaps others, were not formed as $SbCl_6^-$, SO_3F^-, and SO_3Cl^- salts.

Electronic Spectrum of the Bi_5^{3+} Cation. The absorption spectrum of Bi_5^{3+} in molten $NaAlCl_4$ at 130 °C has been reported previously, having been obtained by subtraction of the spectrum of Bi^+ from a composite spectrum of these two cations under the above conditions.[7,8] However, no direct observation of the solution spectrum of Bi_5^{3+} had been made. The preparation of pure $Bi_5(AsF_6)_3 \cdot 2SO_2$ therefore presented an opportunity for the direct observation of the band profile, as well as the calculation of the molar extinction coefficients of the band maxima. Reflectance and mull spectra of solid $Bi_5(AlCl_4)_3$ have also been reported previously,[9] and similar spectra of both $Bi_5(AsF_6)_3 \cdot 2SO_2$ and $Bi_5(AlCl_4)_3$ have been recorded in this work. It should be noted that the solution and solid spectra of Bi_5^{3+} have been claimed to be consistent with a trigonal-bipyramidal structure for this cation.[9]

The band maxima and molar extinction coefficients of the absorption spectrum of $Bi_5(AsF_6)_3 \cdot 2SO_2$ in 100% H_2SO_4 and the reflectance spectrum of the compound are listed in Table I, together with similar data on $Bi_5(AlCl_4)_3$. The Bi_5^{3+} cation was found to be slowly oxidized in 100% H_2SO_4. This was indicated by a complete loss of color after some hours, together with the concomitant formation of a white precipitate. The white material was found to contain only trivalent bismuth. Furthermore, the shoulder at about 275 nm, which is attributed to SO_2, slowly increased in intensity relative to the other bands of the spectrum as the concentration of SO_2 increased as a result of reduction of the sulfuric acid. The values of the molar extinction coefficients therefore represent a lower limit but are estimated to be accurate to ±4%. Attempts to obtain an absorption spectrum of $Bi_5(AlCl_4)_3$ in 100% H_2SO_4 were unsuccessful for reasons of insolubility.

Comparison of the spectra of the hexafluoroarsenate salt with those of the tetrachloroaluminate salt shows that the profiles are very similar and verifies the absorption spectrum of the Bi_5^{3+} cation, as deduced by Bjerrum et al.[7,8] However, the spectrum of the AsF_6^- salt is somewhat better resolved. Thus the band at 425 nm in the solution spectrum of the latter is much more pronounced than the shoulder around 455 nm in the spectrum of the $AlCl_4^-$ salt. Furthermore, a number of striking differences are observed between the spectra of the two compounds. Thus, in both the solid and solution spectra, there is a significant shift of all bands to higher energies in the AsF_6^- salt compared to the $AlCl_4^-$ salt and, in the absorption spectra, there is an approximate threefold decrease in molar absorptivity for the former compound.

The first of the above effects leads to a difference in color between the compounds, so that while $Bi_5(AlCl_4)_3$ is red-brown, $Bi_5(AsF_6)_3 \cdot 2SO_2$ is bright yellow. Also, examination of the reflectance spectra of the two compounds shows that, in addition to the differences in the positions of the band maxima, all bands are somewhat broader in the $AlCl_4^-$ salt, which also contributes to the difference in color.

Fairly recently, a ^{35}Cl NQR study[22] of the $AlCl_4^-$ group in solid $Bi_5(AlCl_4)_3$ gave an unperturbed spectrum for chlorine, showing that the compound is quite "ionic" in nature and that little polarization of the chlorine atoms would be expected. Moreover, strong interactions would not be expected with the smaller, less polarizable and more electronegative fluorine atoms of the AsF_6^- anions or with the H_2SO_4 molecules or HSO_4^- anions in 100% H_2SO_4. The shift in the electronic spectra is therefore probably due to a higher charge density (ionic potential) of the $AlCl_4^-$ anions and, indeed, similar shifts in the electronic spectra of the nitrate anion as a function of cation radius (and hence charge density or ionic potential) in molten nitrate media are well-known.[23]

Vibrational Spectra and Assignments. The most likely structure for the Bi_5^{3+} cation, assuming that it is not polymeric, is either a trigonal bipyramid (D_{3h} symmetry) or a square pyramid (C_{4v} symmetry). The representations of the Raman- and infrared-active normal vibrations for both of these geometries are

$$\Gamma_{vib}\ (D_{3h}) = 2\ A_1' + A_2'' + 2\ E' + E''$$

$$\Gamma_{vib}\ (C_{4v}) = 2\ A_1 + 2\ B_1 + B_2 + 2\ E$$

For the trigonal bipyramid the A_1', E′, and E″ modes are Raman active, while the A_2'' and E′ modes are infrared active. For the square pyramid all modes are Raman active but only the A_1 and E modes are infrared active. Thus, for diagnostic purposes, the totally symmetric vibrations are only Raman active in D_{3h}, but in C_{4v} they are both Raman and infrared active.

The Raman and infrared spectra of $Bi_5(AlCl_4)_3$ and $Bi_5(AsF_6)_3 \cdot 2SO_2$ are reproduced in Figures 1–5, while the positions, relative intensities and assignments of the bands are listed in Table II. The solution spectrum of $Bi_5(AlCl_4)_3$ in $NaAlCl_4$ is shown up to 450 cm^{-1}, and the solid-state spectra are reproduced from about 25 to 150 cm^{-1}. This region covers all fundamental vibrations that are characteristic of the cation. The close similarity between the solid- and liquid-phase Raman spectra for both compounds suggests that the same structure is retained in both phases, while comparison of the spectra with regard to both the number of vibrations and the Raman and

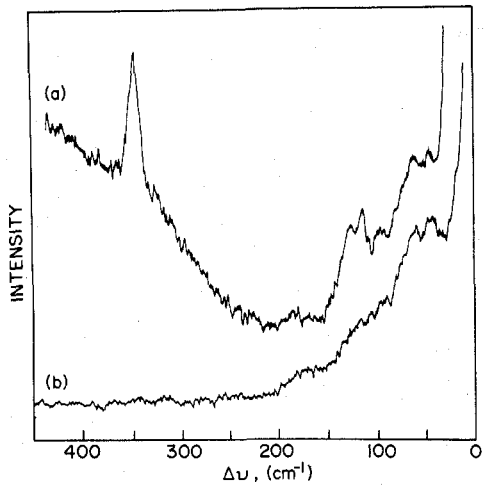

Figure 1. Raman spectra of $Bi_5(AlCl_4)_3$ in molten $NaAlCl_4$ at 180 °C (~6 mol %): (a) incident polarization parallel; (b) incident polarization perpendicular. Exciting line, 5145 Å; power, 750 mW; slit width, 190 μm.

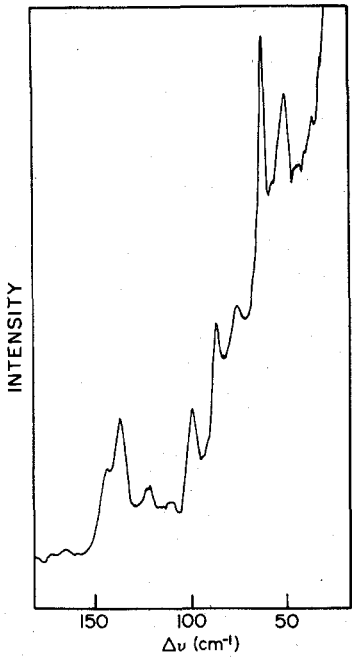

Figure 2. Raman spectrum of solid $Bi_5(AlCl_4)_3$. Exciting line, 6328 Å; power, 68 mW; slit width, 200 μm; rotating sample.

infrared coincidences demonstrates that the Bi_5^{3+} cation has a trigonal-bipyramidal rather than a square-pyramidal structure.

The Raman spectrum of an approximately 6 mol % solution of $Bi_5(AlCl_4)_3$ in molten $NaAlCl_4$ at 180 °C is shown in Figure 1. As one might expect for a spectrum of this type, the bands are fairly broad. However, only five bands can be observed in accord with D_{3h} symmetry, whereas seven would be expected under C_{4v} symmetry. Two totally symmetric modes may be readily identified at 135 and 119 cm^{-1} from polarization measurements. The three remaining bands appear at 97, 62, and 48 cm^{-1}. The positions of the last two bands are somewhat difficult to observe because of their broadness and subsequent overlap, and they are seen most clearly in spectra that were obtained with the polarizer set to 90° (Figure 1b). In the solid-state Raman spectrum of $Bi_5(AlCl_4)_3$ (Figure 2) the totally symmetric vibrations are observed at 146 and 139 cm^{-1} and 125 and 121 cm^{-1}, and in the solid-state Raman spectrum of $Bi_5(AsF_6)_3 \cdot 2SO_2$ (Figure 3) they are observed at 142 and 124 cm^{-1}. In the case of $Bi_5(AlCl_4)_3$ the splitting of the

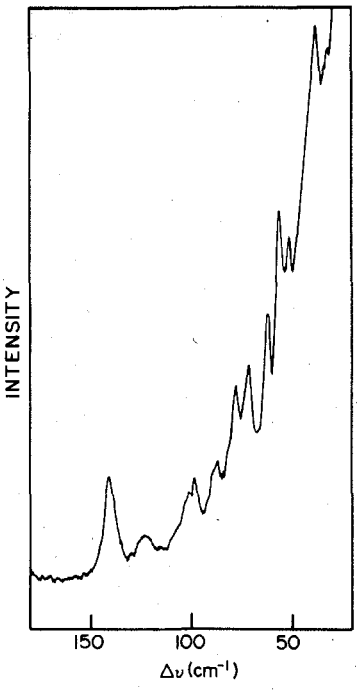

Figure 3. Raman spectrum of solid $Bi_5(AsF_6)_3 \cdot 2SO_2$. Exciting line, 6328 Å; power, 68 mW; slit width, 200 μm; rotating sample.

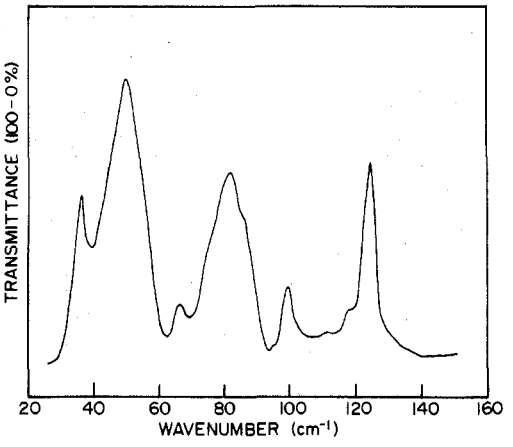

Figure 4. Infrared spectrum of $Bi_5(AlCl_4)_3$ (Nujol mull).

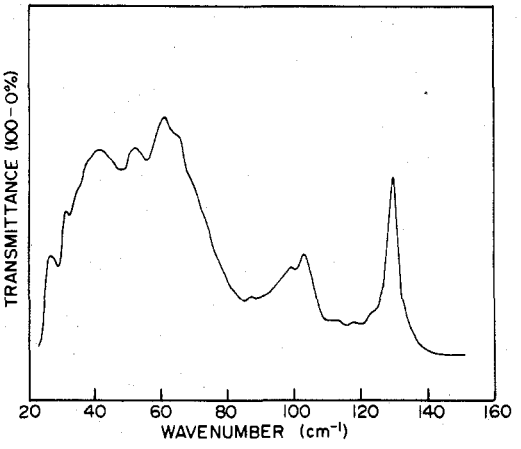

Figure 5. Infrared spectrum of $Bi_5(AsF_6)_3 \cdot 2SO_2$ (Nujol mull).

nondegenerate modes indicates that there is an interaction between the cations in the primitive unit cell, i.e., a factor-group splitting. This is consistent with the lattice parameters for the compound, which has a rhombohedral unit cell with a = 12.21 (5) Å, α = 58.02 (0.27)°, V = 1229 $Å^3$, and two molecules per unit cell. This gives a calculated density of 4.19

Table II. Raman and Infrared Vibrations (cm^{-1}) and Assignments for $Bi_5(AlCl_4)_3$ and $Bi_5(AsF_6)_3 \cdot 2SO_2$

$Bi_5(AlCl_4)_3$			$Bi_5(AsF_6)_3 \cdot 2SO_2$		
solid		solution	solid		
Raman[a]	IR[b]	Raman[a] ($NaAlCl_4$ 180 °C)	Raman[a]	IR[b]	assignment
				27 w	lattice modes
				31 m	
35 (1.3)	36 m				
			42 (6.6)	41 s, br	
43 (0.8)					
51 (4.8)	50 s	48 (1.9) dp	52 (5.2)	52 s	$\nu_5(E')Bi_5^{3+}$
			61 (9.2)	61 s	lattice mode
64 (10.0)	65 w	62 (2.0) dp	64 (8.5)	65 sh, m	$\nu_4(E')Bi_5^{3+}$
			72 (6.5)		lattice modes
77 (1.3)			77 (7.4)		
	82 s				
87 (4.3)	87 sh, m				
			90 (5.9)		
100 (4.0)	100 m	97 (1.2) dp	98 (4.1), 103 (3.8)	98 m, 103 m	$\nu_6(E'')Bi_5^{3+}$
111 (0.7)				115 m	lattice modes
121 (1.3)[c]		119 (4.1) p	124 (1.8)		$\nu_2(A_1')Bi_5^{3+}$
125 (1.3)[c]	125 s, sp			130 s, sp	$\nu_3(A_2'')Bi_5^{3+}$
139 (5.3)[c]		135 (3.6) p	142 (10.0)		$\nu_1(A_1')Bi_5^{3+}$
146 (4.2)[c]					
165 (0.6), 173 (0.3)	165 m	145? (0.5) sh, dp			$\nu_2(E)AlCl_4^-$
183 (0.5), 195 (0.3)	187 s, 193 s	182 (0.9) dp			$\nu_3(F_2)AlCl_4^-$
349 (1.2)		346 (10.0) dp			$\nu_1(A_1)AlCl_4^-$
			365 (1.6)	366 w	$\nu_5(F_{2g})AsF_6^-$
				388 s, 395 s, 404 sh, s	$\nu_4(F_{1u})AsF_6^-$
[d]	459 s				$\nu_4(F_2)AlCl_4^-$
[d]	492 s	[e]			
[d]	527 sh, m				
			683 (4.4)		$\nu_1(A_{1g})AsF_6^-$
				698 s	$\nu_3(F_{1u})AsF_6^-$
			1150 (3.7)	1152 m	$\nu_1(A_1)SO_2$
			1318 (1.2)	~1314 sh, w[f]	$\nu_2(B_1)SO_2$

[a] Relative intensities are given in parentheses. [b] s = strong, m = medium, w = weak, sh = shoulder, br = broad, sp = sharp, p = polarized, dp = depolarized. [c] "Factor-group splitting". See text. [d] Too weak to be observed. [e] Masked by a large fluorescence maximum at ~440 cm^{-1}. See Figure 1. [f] Observed as a shoulder on the Nujol peak at 1380 cm^{-1}.

g cm^{-3}, compared to the measured density of 4.16(5) g cm^{-3} (using 1-bromonaphthalene at 24°C).

No evidence could be found for the appearance of the totally symmetric vibrations in the solid-state infrared spectra of the two compounds (Figures 4 and 5), as would be expected if the cation had C_{4v} symmetry. Conversely, the strong, sharp infrared-active band at 125 cm^{-1} in $Bi_5(AlCl_4)_3$ and at 130 cm^{-1} in $Bi_5(AsF_6)_3 \cdot 2SO_2$ did not appear in the solid-state Raman spectra of the respective compounds, as expected in D_{3h} symmetry. Hence, the observation of the exact number of bands in the Raman solution spectrum for a trigonal bipyramid, together with the lack of infrared activity of the totally symmetric vibrations and the lack of Raman activity of the strong infrared band in the solid-state spectra, shows that the Bi_5^{3+} cation has a trigonal-bipyramidal structure. Using the assignments for an isolated molecule, the totally symmetric vibrations are therefore assigned A_1' symmetry and the strong infrared-active, but Raman-inactive, vibration is assigned A_2'' symmetry. The low-frequency A_1' symmetry mode in the solid-state Raman spectrum of $Bi_5(AlCl_4)_3$ has two components, with the high-frequency component approximately coincident with the A_2'' infrared-active band. Because of the comparable intensity of the two components of the band, this splitting is attributed to a vibrational interaction within the unit cell (factor-group splitting) rather than to the A_2'' band becoming Raman active because of the lowered site symmetry of the cation in the crystalline state.

The bands at 97, 62, and 48 cm^{-1} in the solution spectrum of $Bi_5(AlCl_4)_3$ appear at 100, 64, and 51 cm^{-1} in the solid-state Raman spectrum of $Bi_5(AlCl_4)_3$ and at 103 and 98, 64, and 52 cm^{-1} in the Raman spectrum of $Bi_5(AsF_6)_3 \cdot 2SO_2$. These are all doubly degenerate E′ or E″ modes and in the far-infrared spectrum of $Bi_5(AlCl_4)_3$ they are observed at 100, 65, and 50 cm^{-1} while in $Bi_5(AsF_6)_3 \cdot 2SO_2$ they are observed at 103 and 98, 65, and 52 cm^{-1}. Under strict D_{3h} symmetry the E″ vibration should not be observed in the infrared spectrum, but it appears that because of the lowered site symmetry of the cation in the solid state, this mode becomes infrared active in both compounds. In view of this violation of the symmetry rules, it is not possible to assign these bands to their respective symmetry classes on the basis of the solid-state data. The assignment of the highest frequency mode as E″, making the others E′, is based upon some preliminary infrared data on solutions of $Bi_5(AsF_6)_3 \cdot 2SO_2$ in 100% H_2SO_4 and 98% D_2SO_4 and upon the normal-coordinate analysis.

The spectral work in H_2SO_4 solutions was hampered by the strong absorptions from the "hydrogen-bond stretch" ν(O–H···O) and other low-frequency vibrational modes of the solvent, which extend over a wide range in the far-infrared region. This required the use of very thin films and highly concentrated solutions. Furthermore, as indicated earlier, the Bi_5^{3+} cation is slowly oxidized to Bi(III) in this solvent. After

correction for the solvent, the spectra indicated the presence of a strong band (the A_2'' mode) at 128 cm^{-1} and a strong absorption (the two E′ modes) from about 65 to 55 cm^{-1}. No band was observed around 100 cm^{-1}, indicating that the vibrations observed from 99 to 103 cm^{-1} in the solid-state spectra originally arise from the E″ mode. Also, alternative band assignments, using all of the geometries discussed below, gave unreasonable values for the primary stretching and interaction force constants and in many cases an interaction force constant of comparable magnitude to, or even greater than, the smaller of the two primary stretching force constants.

The bands at 100 cm^{-1} in $Bi_5(AlCl_4)_3$ and at 103 and 98 cm^{-1} in $Bi_5(AsF_6)_3 \cdot 2SO_2$ are therefore assigned E″ symmetry, with the band in the hexafluoroarsenate salt being split. The bands at 64–65 cm^{-1} in $Bi_5(AlCl_4)_3$ and $Bi_5(AsF_6)_3 \cdot 2SO_2$ are assigned E′ symmetry and appear to be of low intensity in the far-infrared spectrum. The stronger intensity in the case of the hexafluoroarsenate salt appears to arise from an exceptionally strong lattice vibration at 61 cm^{-1}, so that the fundamental appears as a shoulder on this vibration in the far-infrared spectrum. The lattice mode also appears in the Raman spectrum of this compound, but as the bands are so much sharper, there is no overlap of the fundamental and lattice vibrations. The remaining bands at 50–51 cm^{-1} in $Bi_5(AlCl_4)_3$ and at 52 cm^{-1} in $Bi_5(AsF_6)_3 \cdot 2SO_2$ are assigned E′ symmetry.

All other bands may be attributed to lattice modes, to anion bands, or to SO_2, and assignments were made by analogy with previous assignments. As pointed out above, the splitting of the two A_1' modes in $Bi_5(AlCl_4)_3$ indicates that there is some vibrational interaction between the cations in the unit cell, i.e., a factor-group splitting. However, because of the lack of definitive crystallographic information on this compound, no attempt was made to analyze the spectra in more detail. It should also be noted that in solid $Bi_5(AlCl_4)_3$ both ν_3 (F_2) and ν_4 (F_2) for the $AlCl_4^-$ anion are split and ν_2 (E) is probably split as well, but because of overlap with other bands, it is difficult to observe the components of this mode. Similarly, the ν_4 (F_{1u}) mode of the AsF_6^- anion in $Bi_5(AsF_6)_3 \cdot 2SO_2$ is split and the ν_5 (F_{2g}) mode, which is Raman active but infrared inactive under full O_h symmetry, appears as a weak band in the infrared spectrum of this compound. There would, therefore, seem to be considerable evidence of site and factor-group effects in these compounds, probably involving distortion of the anions from cubic symmetry.

Vibrational Analysis. The assignments for the Raman- and infrared-active bands of the Bi_5^{3+} cation indicate that the cation has a trigonal-bipyramidal structure, and a vibrational analysis was made on this basis.

The **F** and **G** matrices for trigonal-bipyramidal Bi_5^{3+} (point group D_{3h}) were constructed according to the methods described by Wilson, Decius, and Cross,[24] using the computer programs EXCART, GBMMOD, and FGZSYM.[25] All Bi–Bi distances were initially set at 3.04 Å as suggested by the X-ray radial-distribution analysis of both liquid and powdered samples of "$BiAlCl_4$".[26] According to the phase diagram for the $Bi–BiCl_3–3AlCl_3$ system, material of this composition contains five-sixths of the metal as $Bi_5(AlCl_4)_3$, with the remaining bismuth in the tripositive oxidation state.[9] The results of the X-ray study suggested the presence of triangular Bi_3 (D_{3h}) units, which may presumably be identified with the triangular faces of a trigonal bipyramid having Bi–Bi distances of 3.04 Å.

Stretches along the nine edges of a trigonal bipyramid conveniently form a complete set of internal coordinates and may be used to describe the vibrational motion. These are illustrated in Figure 6. The symmetry coordinates formed from these internal coordinates, listed in Table III, were used

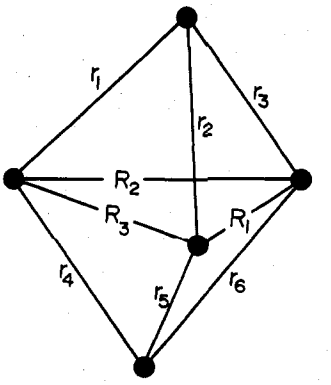

Figure 6. Geometry and arrangement of the internal coordinates for a trigonal bipyramid (D_{3h}); r is the equilibrium axial Bi–equatorial Bi distance and R is the equilibrium equatorial Bi–equatorial Bi distance.

Table III. Symmetry Coordinates for Bi_5^{3+}

A_1'

$$S_r(A_1') = (1/6^{1/2})(r_1 + r_2 + r_3 + r_4 + r_5 + r_6)$$
$$S_R(A_1') = (1/3^{1/2})(R_1 + R_2 + R_3)$$

A_2''

$$S_r(A_2'') = (1/6^{1/2})(r_1 + r_2 + r_3 - r_4 - r_5 - r_6)$$
$$S_R(A_2'') = 0 \quad (R \text{ does not contribute to } A_2'')$$

E′

$$S_{r_1}(E') = (1/12^{1/2})(2r_1 - r_2 - r_3 + 2r_4 - r_5 - r_6)$$
$$S_{r_2}(E') = (1/2)(r_2 - r_3 + r_5 - r_6)$$
$$S_{R_1}(E') = (1/6^{1/2})(2R_1 - R_2 - R_3)$$
$$S_{R_2}(E') = (1/2^{1/2})(R_2 - R_3)$$

E″

$$S_{r_1}(E'') = (1/12^{1/2})(2r_1 - r_2 - r_3 - 2r_4 + r_5 + r_6)$$
$$S_{r_2}(E'') = (1/2)(r_2 - r_3 - r_5 + r_6)$$
$$S_R(E'') = 0 \quad (R \text{ does not contribute to } E'')$$

in the program FGZSYM to symmetrize the **G** and **F** matrices.

For a trigonal bipyramid, the generalized valence force field (GVFF) requires eight independent force constants, including both primary stretching and interaction force constants. This may be expressed as

$$2V = F_r\sum^{6}\Delta r_{ij}^2 + F_R\sum^{3}\Delta R_{ij}^2 + 2F_{rr}\sum^{6}\Delta r_{ij}\Delta r_{ik} + 2F_{rr}'\sum^{3}\Delta r_{ij}\Delta r_{jl} + 2F_{rr}''\sum^{6}\Delta r_{ij}\Delta r_{kl} + 2F_{rR}\sum^{12}\Delta r_{ij}\Delta R_{jk} + 2F_{rR}'\sum^{6}\Delta r_{ij}\Delta R_{kl} + 2F_{RR}\sum^{3}\Delta r_{ij}\Delta R_{jk}$$

where the force constants are defined in Table IV and Δr_{ij} and Δ_{Rij} represent changes in the equilibrium distances between the ith and jth atoms ($i, \ldots, l = 1, \ldots, 5$). As there are only six vibrational pieces of information and as isotopic replacement would not give rise to measurable shifts in the frequencies of the normal modes of vibration, a number of modified force fields were investigated. These various force fields are discussed below, but all are expressed in terms of the force constants of the GVFF, as given in Table IV. Solution of the secular equation was carried out by computer using the program GFPP.[25]

The first potential field that was attempted assumed that the primary stretching force constants, F_r and F_R, were equal and that $F_{rr} = F_{rR} = F_{RR}$. This field, therefore, required only five force constants. All other force constants were assumed to be zero. However, no adequate fit to the data could be obtained, even when any one of the interaction force constants was allowed to vary independently of the other two, thereby

Table IV

Vibrational Calculations for the Bi_5^{3+} Cation

	frequencies, cm^{-1}		
		calcd	
species	obsd[a]	geometry A	geometries B and C (I and II)
A_1'	142	142.4	142.0
	124	123.5	124.0
A_2''	128	127.9	128.0
E'	65	65.4	65.0
	51	50.8	51.0
E''	101	101.1	101.0

Force Constants (mdyn/Å) for the Bi_5^{3+} Cation

force constant[b]	geometry A	geometry B	geometry C	
			I	II
F_r	0.747	0.729	0.727	0.698
F_R	0.525	0.526	0.553	0.592
F_{rr}	0.089[c]	0.113	0.128	0.098
F_{rr}'	0.089[c]	0.047	0.029	0.000[d]
F_{rr}''	0.116	0.126	0.131	0.101
F_{rR}	−0.203	−0.185[c]	−0.192[c]	−0.186
F_{rR}'	0.000[d]	0.000[d]	0.000[d]	0.000[d]
F_{RR}	0.183	0.185[c]	0.192[c]	0.239

[a] Mean values taken from all solid-state spectra. [b] F_r, axial-equatorial Bi-Bi stretch; F_R, equatorial-equatorial Bi-Bi stretch; F_{rr}, stretch-stretch interaction between two axial-equatorial stretches in the same tetrahedron; F_{rr}', stretch-stretch interaction between two axial-equatorial stretches in different tetrahedra, connected by an equatorial Bi atom; F_{rr}'', stretch-stretch interaction between two axial-equatorial stretches in different tetrahedra, not connected by a Bi atom; F_{rR}, stretch-stretch interaction between an axial-equatorial and an equatorial-equatorial stretch, connected by an equatorial Bi atom; F_{rR}', stretch-stretch interaction between an axial-equatorial and an equatorial-equatorial stretch, not connected by a Bi atom; F_{RR}, stretch-stretch interaction between two equatorial-equatorial stretches. [c] Assumed equal to, or the negative of, each other in the force field. [d] Constrained to zero in the force field.

extending the field to six force constants.

The force field was then altered so the F_r and F_R were no longer equal. All interaction force constants were allowed to vary independently with the exception that interaction force constants between two Bi–Bi stretches with no atoms in common (F_{rr}'' and F_{rR}') were placed equal to zero, giving six independent force constants in all. Once again no satisfactory solution could be obtained, for although five frequencies could be fitted with this force field, the value calculated for the A_2'' mode was always much higher than the experimental value. Examination of the symmetrized **F** matrix showed that F_{rr}'' made a significant contribution to this mode and suggested that in this geometry, as also found for other cage and cluster compounds such as P_4,[27] interaction force constants between two stretches that have no atoms in common are quite important. Indeed, these are often observed to be of similar magnitude to the other interaction force constants.

The potential field was then changed to take into account at least one force constant of the type described above (usually F_{rr}'') and two interaction force constants were constrained such that they were equal to each other, again giving a field of six independent force constants. While every possible combination was not investigated, only one solution of this type was obtained, that with $F_{rR}' = 0$ and $F_{rr} = F_{rr}'$. The results of this calculation are given in Table IV and the potential energy distribution (Table V) shows that, as one might expect, there is considerable mixing of the internal coordinates in the normal modes of vibration, even with this simplified force field.

Although the above solution may not be unique, in every case the primary stretching force constants approached similar values to those given in Table IV and only the interaction force constants were found to change. Similar agreement would probably occur with any other possible solution, leaving the primary force constants essentially unaltered.

As indicated earlier, all Bi–Bi distances were initially set at 3.04 Å, based upon the assumption that the Bi_5^{3+} cation has a trigonal-bipyramidal structure with all edges equal in length; i.e., it consists of two tetrahedra sharing a face. The isovalent Pb_5^{2-} and Sn_5^{2-} anions, however, do not have such a regular structure but instead have trigonal-bipyramidal structures with shorter axial–equatorial than equatorial–equatorial edge distances.[28,29] In the case of the isoelectronic Pb_5^{2-} anion these are 3.002 and 3.238 Å, respectively. This gives a weighted average Pb–Pb distance of 3.08 Å for the trigonal bipyramid, slightly larger than the (average?) Bi–Bi

Table V. Potential Energy Distribution for the Bi_5^{3+} Cation

			V_{ij}[a]							
species	freq, cm^{-1}	geometry	V_r	V_R	V_{rr}	V_{rr}'	V_{rr}''	V_{rR}	V_{rR}'[b]	V_{RR}
A_1'	142	A	63	0	15	8	20	−6	0	0
		B	77	19	24	5	26	−64	0	13
		C I	75	29	26	0	27	−80	0	20
		C II	38	69	11	0[b]	11	−84	0	56
A_1'	124	A	22	84	5	0	7	−78	0	58
		B	0	59	0	0	0	0	0	41
		C I	0	50	0	0	0	14	0	34
		C II	46	0	13	0[b]	13	22	0	0
A_2''	128	A	124	0	29	−15	−38	0	0	0
		B	111	0	34	−7	−38	0	0	0
		C I	105	0	37	0	−38	0	0	0
		C II	101	0	28	0[b]	−29	0	0	0
E'	65	A	126	0	−15	15	−20	−7	0	0
		B	147	0	−23	9	−25	−9	0	0
		C I	135	0	−24	5	−24	7	0	0
		C II	139	0	−20	0[b]	−20	0	0	0
E'	51	A	65	247	−8	8	−10	−116	0	−86
		B	70	245	−11	0	−12	−110	0	−86
		C I	113	258	−20	5	−20	−146	0	−89
		C II	92	277	−13	0[b]	−13	−131	0	−112
E''	101	A	109	0	−13	−13	17	0	0	0
		B	105	0	−16	−7	18	0	0	0
		C I	104	0	−18	0	19	0	0	0
		C II	100	0	−14	0[b]	14	0	0	0

[a] Contributions to the potential energy of less than 5% are not included in the table. [b] Not included in the potential field.

distance of 3.04 Å found from the X-ray radial-distribution analysis. The G matrix was therefore reconstructed using axial–equatorial and equatorial–equatorial Bi–Bi distances of 2.962 and 3.195 Å, respectively, calculated on the basis of the Pb_5^{2-} anion geometry and a weighted average of 3.04 Å. Attempts to obtain a solution using the above force field were unsuccessful. The potential field was therefore modified and a solution was achieved with $F_{rR}' = 0$ and $F_{rR} = -F_{RR}$. The force constants and potential energy distribution using this potential field are also given in Tables IV and V (geometry B) and are similar to the values calculated using the original potential field.

If it is assumed that the cation has shorter axial–equatorial than equatorial–equatorial edge distances, as found in the Pb_5^{2-} and Sn_5^{2-} anions, then an alternative interpretation of the original X-ray radial-distribution analysis may be made. The peak at 3.04 Å is very close to the nearest-neighbor distance of 3.071 Å found in bismuth metal[30] and probably represents a lower limit to any Bi–Bi distance in the cation. It is, therefore, suggested that this value is the axial–equatorial distance and that the equatorial–equatorial distance is coincident with the rather broad, lower intensity peak at 3.4 Å, which was originally assigned as the Bi–Cl distance. This is not unreasonable as the equatorial–equatorial distance peak should have only half the intensity of the axial–equatorial peak. Furthermore, the weighted average Bi–Bi distance is then 3.15 Å, which is close to the weighted average distance of 3.14 Å found for Bi_9^{5+}, taken over all of the reasonable bonding distances in this cation (3.0–3.3 Å).[6] Both cations show a comparable formal oxidation state for bismuth, +0.60 in Bi_5^{3+} and +0.56 in Bi_9^{5+}. The G matrix was reconstructed using this geometry, and the force constants and potential energy distribution, employing the second of the force fields discussed above, are listed in Tables IV and V (geometry C, calculation I). These appear little different from the previous calculation (geometry B). A second solution to the problem was also obtained by constraining $F_{rr}' = 0$, again with $F_{rR}' = 0$. In this case only six independent force constants are required in the potential field. The data are given as above (geometry C, calculation II) and it may be noted that F_r and F_R are now closer in magnitude, while some variations in the contribution to the potential energy distribution have occurred.

Comparison of the stretching force constants for the axial–equatorial and equatorial–equatorial Bi–Bi stretches in any of the three geometries indicates that the former (~0.73 mdyn/Å) is considerably larger than the latter (~0.55 mdyn/Å) and reflects the higher bond order of the axial–equatorial Bi–Bi bond. This result is consistent with both valence bond and MO bonding treatments for the cation. In terms of simple valence bond ideas, the Bi_5^{3+} cation can best be described by several resonance structures involving six two-electron, two-center bonds with either a lone pair or an "inert" $6s^2$ core on each bismuth atom. Thus, there is one resonance structure of type **1**, twelve of type **2**, including

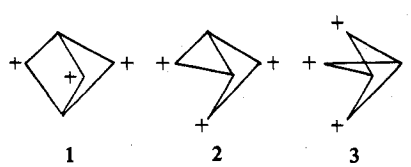

1 **2** **3**

reflection through the plane containing the equatorial atoms, and three of type **3**. In "electron-deficient" molecules such as these, this leads to formal bond orders of less than 1 and in this case to a higher axial–equatorial than equatorial–equatorial bond order. Such descriptions involving localized two-center bonds are, however, not particularly informative and these systems are best treated in terms of an LCAO–MO approach.

Table VI. Bond Distances, Force Constants, and Population Matrices for the Axial–Equatorial and Equatorial–Equatorial Bi–Bi Separations

	axial–equatorial separation			equatorial–equatorial separation		
geometry	bond distance, Å	force constant, mdyn/Å	population matrix	bond distance, Å	force constant, mdyn/Å	population matrix
A	3.04	0.747	0.251	3.04	0.525	0.172
B	2.962	0.729	0.268	3.195	0.526	0.150
C I	3.04	0.727	0.264	3.40	0.553	0.129
C II	3.04	0.698	0.264	3.40	0.592	0.129

An extended-Hückel MO treatment of the Bi_5^{3+} cation[31] was also found to be consistent with the results of the force-constant analysis, as shown below. This MO treatment included all overlap but involved only the 6p orbitals as a basis set. The 6s orbitals were regarded as filled, thereby providing an "inert core" on each atom. Justification for such a simple treatment is provided by the considerable 6s–6p and 6p–6d separations for bismuth. The results of the study indicated that the trigonal-bipyramidal structure, using each of the geometries discussed above, could accommodate the 12 bonding electrons in a closed-shell configuration $[(A_1')^2(A_2'')^2(E')^4(E'')^4]$ with a large gap to the lowest antibonding MO (2 E').[32] Examination of the population matrix, which is defined as $2S_{ij}\sum c_i c_j$, the sum being over all of the occupied MO's, provides an idea of the bonding and charge distribution in the cation. When taken over all of the relevant combinations of AO's, this matrix reflects the difference in bond order of the axial–equatorial and equatorial–equatorial "bonds". The values of the bond distances, force constants, and population matrices for the axial–equatorial and equatorial–equatorial Bi–Bi separations for all three geometries are given in Table VI. Qualitative agreement is observed in each case. This is most gratifying in view of the simplifications inherent in the MO calculations and because, in the normal-coordinate analysis, as angle bending coordinates are redundant with stretching coordinates, the primary force constants are really composite force constants which pertain to deformation motions as well as stretching motions.

The population matrix also indicates that in geometries A and B the orbitals on the axial atoms are somewhat more occupied than those on the equatorial atoms, such that there is an approximately uniform electron distribution around each atom. This implies that the cationic charge is spread evenly over all of the atoms of the cluster (+0.600/atom). However, in geometry C, the electron distribution is such that the equatorial atoms carry slightly more of the cationic charge (+0.623/atom) compared to the axial atoms (+0.556/atom). Thus in terms of the simple valence bond ideas discussed above, resonance structures **2** and **3** obviously play an important role in a description of the cation. It is also of interest to note that the interaction force constants, particularly F_{rR} and R_{RR}, are quite significant. This may be rationalized in terms of electron redistribution during the antisymmetric vibrations and may be correlated with the contributions of the various resonance forms in a valence-bond description of the cation. A more complete discussion of the MO treatment, including similar descriptions of the isovalent Pb_5^{2-} and Sn_5^{2-} anions, is given in another paper.[31]

Very few Bi–Bi stretching force constants are available for comparison with our values of ~0.73 and ~0.55 mdyn/Å. The force constant for the $^{209}Bi_2$ molecule is 1.84 mdyn/Å, as calculated from data derived from the emission-band spectrum of gaseous bismuth metal.[33] However, considerable multiple bonding would be expected in this molecule, as is reflected in the higher stretching force constant. The only other example is the stretching force constant that has been

used to account for the three cluster-type Raman bands in the $Bi_6(OH)_{12}^{6+}$ cation.[34] This cation contains an octahedron of bismuth atoms with the hydroxide groups lying over the octahedral edges of the cluster. The Bi–Bi distance is 3.71 Å. In this case the stretching force constant was found to be ~0.97 mdyn/Å, and it was suggested that evidence for the proposed bismuth–bismuth bonding was supported by the anomalously high intensity of the low-frequency Raman bands attributable to the octahedron of bismuth atoms. Here, the relatively high stretching force constant, considering the rather large Bi–Bi separation, reflects the simplified potential field which has only a single force constant related to the bismuth cage.

It is also of interest to apply the central force field approximation to Bi_5^{3+} (with no interaction between the axial atoms). In this potential field the **F** matrix contains no cross terms but instead only diagonal terms. Therefore only two force constants (F_r and F_R) are required in this description. Assuming that the two force constants are equal in magnitude, then the ratios and ordering of frequencies in the cluster can be predicted from an examination of the diagonal elements of the symmetrized **G** matrix. If the two force constants are not equal, then variations from these ratios will occur. Incorporation of the off-diagonal terms, which are actually quite significant, will also contribute to the variations that are observed. For Bi_5^{3+} with geometry C, the ratios $\nu_1:\nu_3:\nu_2:\nu_6:\nu_4:\nu_5$ are 2.06:2.00:1.77:1.23:1.03:1.00. The ordering of frequencies is as found experimentally, but all ratios are smaller than observed. In the case of geometries A and B, the order is essentially that given above, except that ν_3 (A_2'') is predicted to be higher than ν_1 (A_1'). On increasing the equatorial–equatorial distance relative to the axial–equatorial distance, ν_3 approaches ν_1 until, as in geometry C, ν_1 is greater than ν_3.

The reason that the order of frequencies closely approximates that given by a consideration of the symmetrized **G** matrix in this case stems from the relatively high symmetry of the cluster and the high atomic masses of the atoms concerned, there being little anharmonicity in their vibrations. As such, the ordering and relative ratios of the diagonal **G** matrix elements provide some help in the assignment of the vibrational bands of a homoatomic cluster, especially for those that contain heavy atoms. This procedure has been used to infer the presence of clusters containing three (D_{3h}), four (T_d) and six (O_h) atoms in transition-metal and post-transition-metal compounds.[35]

Finally, of the three geometries proposed for the Bi_5^{3+} cation, geometries B and C are obviously more realistic than geometry A in view of the recently reported structures of the Pb_5^{2-} and Sn_5^{2-} anions. Furthermore, it is expected that geometry C will be closer to the true geometry of the Bi_5^{3+} cation based, first, on the alternative interpretation of the X-ray radial-distribution analysis presented earlier and, second, on the identical agreement of the observed ordering of frequencies with that predicted for this geometry using the simple cluster procedure described above.

Acknowledgment. We thank Professor J. D. Corbett for his suggestions concerning the interpretation of the electronic spectra of Bi_5^{3+} in different media and we thank Dr. T. Timusk and Mr. H. Navarro, of the Department of Physics, at this University, for obtaining some of the far-infrared data reported in this paper.

Registry No. $Bi_5(AsF_6)_3$, 68002-15-3; $Bi_5(AlCl_4)_3$, 12301-55-2.

References and Notes

(1) L. E. Topol, S. J. Yosim, and R. A. Osteryoung, *J. Phys. Chem.*, **65**, 1511 (1961).
(2) C. R. Boston and G. P. Smith, *J. Phys. Chem.*, **66**, 1178 (1962).
(3) C. R. Boston, G. P. Smith, and L. C. Howick, *J. Phys. Chem.*, **67**, 1849 (1963).
(4) J. D. Corbett, *J. Am. Chem. Soc.*, **80**, 4757 (1958).
(5) A. Hershaft and J. D. Corbett, *Inorg. Chem.*, **2**, 979 (1963).
(6) R. M. Friedman and J. D. Corbett, *Inorg. Chem.*, **12**, 1134 (1973).
(7) N. J. Bjerrum, C. R. Boston, G. P. Smith, and H. L. Davis, *Inorg. Nucl. Chem. Lett.*, **1**, 141 (1965).
(8) N. J. Bjerrum, C. R. Boston, and G. P. Smith, *Inorg. Chem.*, **6**, 1162 (1967).
(9) J. D. Corbett, *Inorg. Chem.*, **7**, 198 (1968).
(10) R. J. Gillespie and J. Passmore, *Chem. Commun.*, 1333 (1969).
(11) R. J. Gillespie and P. K. Ummat, *Can. J. Chem.*, **48**, 1239 (1970).
(12) R. J. Gillespie, W. Luk, and D. R. Slim, *J. Chem. Soc., Chem. Commun.*, 791 (1976).
(13) P. Boldrini, I. D. Brown, R. J. Gillespie, P. R. Ireland, W. Luk, D. R. Slim, and J. E. Vekris, *Inorg. Chem.*, **15**, 765 (1976).
(14) R. J. Gillespie, W. Luk, E. Maharajh, and D. R. Slim, *Inorg. Chem.*, **16**, 892 (1977).
(15) R. J. Gillespie and P. K. Ummat, *Inorg. Chem.*, **11**, 1674 (1972).
(16) J. Barr, R. J. Gillespie, R. Kapoor, and K. C. Malhotra, *Can. J. Chem.*, **46**, 149 (1968).
(17) J. Barr, Ph.D. Thesis, McMaster University, 1959.
(18) P. A. W. Dean, R. J. Gillespie, and P. K. Ummat, *Inorg. Synth.*, **25**, 213–222 (1974).
(19) J. D. Corbett, *Prog. Inorg. Chem.*, **21**, 129–158 (1976).
(20) H. A. Levy, P. A. Agron, M. D. Danford, and R. D. Ellison, *Acta Crystallogr.*, **14**, 549 (1961).
(21) A. F. Reid, D. E. Scaife, and P. C. Wailes, *Spectrochim. Acta, Part A*, **20a**, 1257 (1964).
(22) D. J. Merryman, P. A. Edwards, J. D. Corbett, and R. E. McCarley, *Inorg. Chem.*, **13**, 1471 (1974).
(23) See, for example, D. M. Gruen, *Q. Rev., Chem. Soc.*, **19**, 349 (1965), and references therein.
(24) E. B. Wilson, J. C. Decius, and P. C. Cross, "Molecular Vibrations", McGraw-Hill, New York, N.Y., 1955.
(25) The computer programs EXCART, GBMMOD, FGZSYM, and GFPP were written by J. H. Schachtschneider, Technical Report No. 9032-VII, of the Shell Development Co., 1965, and modified by W. V. F. Brooks in 1968, then at Ohio University, now at The University of New Brunswick. The programs were obtained from H. F. Shurvell of Queen's University and subsequently modified by G. Turner of McMaster University to run on a CDC 6400 computer.
(26) H. A. Levy, M. A. Bredig, M. D. Danford, and P. A. Agron, *J. Phys. Chem.*, **64**, 1959 (1960).
(27) C. W. F. T. Pistorius, *J. Chem. Phy.*, **29**, 1421 (1958).
(28) J. D. Corbett and P. A. Edwards, *J. Chem. Soc., Chem. Commun.*, 984 (1975).
(29) P. A. Edwards and J. D. Corbett, *Inorg. Chem.*, **16**, 903 (1977).
(30) P. Cucka and C. S. Barret, *Acta Crystallogr.*, **15**, 865 (1962).
(31) R. C. Burns, R. J. Gillespie, and M. J. McGlinchey, in preparation.
(32) The ordering of the molecular orbitals for Bi_5^{3+} in all of the three geometries is A_1', A_2'', E', E'', 2 E', A_2', 3 E', 2 A_1', 2 A_2'', 2 E''.
(33) G. Herzberg, "Molecular Spectra and Molecular Structure, I. Spectra of Diatomic Molecules", 2nd ed., Van Nostrand, Princeton, N.J., 1950, p 510.
(34) V. A. Marconi and T. G. Spiro, *Inorg. Chem.*, **7**, 183 (1968).
(35) T. G. Spiro, *Prog. Inorg. Chem.*, **11**, 1–51 (1970).